



# Clear Detection of Thin-Walled Regions in Unruptured Cerebral Aneurysms by Using Computational Fluid Dynamics

Kimura, Hidehito ; Taniguchi, Masaaki ; Hayashi, Kosuke ; Fujimoto, Yosuke ; Fujita, Youichi ; Sasayama, Takashi ; Tomiyama, Akio ;...

---

(Citation)

World Neurosurgery, 121:e287-e295

(Issue Date)

2019-01

(Resource Type)

journal article

(Version)

Accepted Manuscript

(Rights)

© 2019 Elsevier Inc.

This manuscript version is made available under the CC-BY-NC-ND 4.0 license  
<http://creativecommons.org/licenses/by-nc-nd/4.0/>

(URL)

<https://hdl.handle.net/20.500.14094/90007040>



Title: Clear Detection of Thin-Walled Regions in Unruptured Cerebral Aneurysms by Using  
Computational Fluid Dynamics

Authors:

Hidehito Kimura, M.D., Ph.D. <sup>\*1</sup>; Masaaki Taniguchi, M.D., Ph.D. <sup>\*1</sup>; Kosuke Hayashi, D.Eng. <sup>\*2</sup>;  
Yosuke Fujimoto, M.D. <sup>\*1</sup>; Youichi Fujita, M.D. <sup>\*1</sup>; Takashi Sasayama, M.D., Ph.D. <sup>\*1</sup>; Akio  
Tomiyama, D.Eng. <sup>\*2</sup>; Eiji Kohmura, M.D., Ph.D. <sup>\*1</sup>

Affiliation:

Department of Neurosurgery, Kobe University Graduate School of Medicine, Kobe, Japan <sup>\*1</sup>

Kobe University Graduate School of Engineering, Kobe, Japan <sup>\*2</sup>

Corresponding author:

Hidehito Kimura

Department of Neurosurgery, Kobe University Graduate School of Medicine

7-5-1, Kusunoki-cho, Chuo-ku, Kobe, 650-0017, JAPAN

1 Tel.: +81-78-382-5966, Fax: +81-78-382-5979

2 E-mail: [hkimura@med.kobe-u.ac.jp](mailto:hkimura@med.kobe-u.ac.jp)

3

4 Key words:

5 cerebral aneurysm, computational fluid dynamics, wall shear stress vector cycle variation, wall

6 thinning, visualization

7

## 1    **ABSTRACT**

2    Objective: The thin-walled regions (TIWRs) within cerebral aneurysms have a high risk of rupture  
3    during surgical manipulation. Previous reports have demonstrated specific changes in the  
4    computational fluid dynamics (CFD) parameters at TIWRs but have not been fully evaluated. We  
5    identified a novel parameter, wall shear stress vector cycle variation (WSSVV), with user-friendly  
6    software that could predict TIWRs and investigated.

7    Methods: Twelve unruptured cerebral aneurysms were analyzed. TIWRs were defined as reddish  
8    areas compared with the normal-colored parent artery on intraoperative views. The position and  
9    orientation of these clinical images were adjusted to match the WSSVV color maps. TIWRs and  
10   thick-walled regions (TKWRs) were marked and compared with the corresponding regions on  
11   WSSVV maps. The default images obtained from WSSVV imaging required appropriate  
12   maximum color bar value (MCBV) adjustment for predicting TIWRs. Sensitivity and specificity  
13   analyses were performed by changing the MCBV from 300 to 700 at intervals of 100. With the  
14   optimal MCBV, WSSVV values were quantitatively compared.

15   Results: All 18 TIWRs and all 16 TKWRs selected corresponded to low- and high-value regions  
16   of the WSSVV color maps at the adjusted MCBV, respectively. The mean optimal MCBV was

- 1     $483.3 \pm 167.50$  (range: 300 -700). According to receiver-operating characteristic (ROC) analysis,
- 2    the best MCBV for predicting TIWRs was 500 (highest rate of sensitivity, 0.89; specificity, 0.94).
- 3    Under this condition, the quantitative values of the CFD color maps for TIWRs and TKWRs were
- 4    significantly different ( $p < 0.01$ ).
- 5    Conclusion: Low WSSVV values may indicate TIWRs within cerebral aneurysms.

## 1 INTRODUCTION

2 Intraoperative aneurysm rupture is associated with high rates of mortality and morbidity during  
3 microsurgical clipping or endovascular coiling<sup>1,2</sup>. Aneurysm rupture is thought to occur at thin-  
4 walled regions (TIWRs), which have high potential risks of rupture during surgical manipulation<sup>3</sup>.  
5 <sup>4</sup>. During endovascular coiling, visualization of TIWRs or rupture points is impossible; thus, the  
6 possible reasons for intraoperative ruptures are unknown<sup>5, 6</sup>. A better preoperative understanding  
7 of the locations of TIWRs within aneurysms, not only during clipping but also during coiling, will  
8 help shape the surgical strategy and increase the safety of the surgical procedure. Although the  
9 imaging modalities for evaluating cerebral aneurysms have improved recently, these methods are  
10 still unable to accurately evaluate the condition of the aneurysm wall<sup>5, 7</sup>.

11 Using recently advanced computational fluid dynamics (CFD) tools, a few reports have  
12 estimated aneurysm wall conditions (thick or thin walls) by comparing CFD findings to  
13 intraoperative microsurgical observations of the aneurysm dome<sup>8-9</sup>. Regarding wall shear stress  
14 (WSS), which is a representative parameter of CFD, Kadasi et al. reported that low WSS correlated  
15 with TIWRs<sup>10</sup>. In contrast, Suzuki et al. reported that high WSS correlated with TIWRs<sup>11</sup>. In

another study, Sugiyama et al. reported that atherosclerotic changes within the aneurysm sacs were equivalent to thick-walled regions (TKWRs), and these regions had low WSS values<sup>12</sup>. Therefore, using WSS to predict TIWRs remains controversial. Other parameters that have been used to predict TIWRs and TKWRs include pressure differences and relative residence times (RRTs)<sup>11-9</sup>. However, no single parameter can effectively predict aneurysm wall conditions. Furthermore, the required diagnostic tools are professional and are not ready for clinical use.

We investigated the factors corresponding to TIWRs within the aneurysm dome by analyzing hemodynamic parameters with the commercially available software Hemoscope Ver1.5 (EBM Corp., Tokyo, Japan) (which can be easily managed by clinicians). We found that low WSS vector cycle variation (WSSVV), representing an unique hemodynamic index calculated by Hemoscope, may correspond to TIWRs.

The purpose of this study was to verify these findings by comparing the distributions of TIWRs within unruptured cerebral aneurysms (identified via intraoperative microscopic views) with the distributions of WSSVV or time-averaged WSS (TAWSS) from CFD maps and to evaluate whether WSSVV or TAWSS are reliable predictors of TIWRs within cerebral aneurysms.

## 1   **METHODS**

### 2   Patient Selection

3       This was a retrospective study. Between April 2013 and March 2017, a total of 526 patients  
4   with unruptured intracranial aneurysms were referred to our institute. Among the referred  
5   patients, 66 had undergone neck clipping to prevent rupture in accordance with the relevant  
6   guidelines. From these patients, we selected 12 aneurysms that met the following inclusion  
7   criteria: 1) saccular aneurysm treated by direct surgery, 2) patient age between 20 and 90 years,  
8   3) aneurysm surface could be observed clearly under microscopy, 4) red thin walls detected on  
9   the dome by microsurgical observation, and 5) available preoperative high-resolution 3-  
10   dimensional computed tomography angiography (3D-CTA) data. Three men and 9 women were  
11   included (mean age,  $61.0 \pm 9.79$  years; mean aneurysm size,  $6.27 \pm 1.19$  mm), with 6 aneurysms in  
12   the middle cerebral artery (MCA), 5 aneurysms in the internal carotid artery (ICA) and one  
13   aneurysm in the vertebral artery (VA) (Table 1). Aneurysms that were dissected, fusiform, or  
14   clipped after coil embolization were excluded. Ruptured aneurysms were also excluded because  
15   of impaired visualization of the aneurysm wall.



The study was conducted in accordance with the guidelines and with the approval of the local ethics committee of our institution, and written informed consent was obtained from all patients.

#### Intraoperative Video

Intraoperative video recording was performed in all cases by using a surgical microscope, namely, a Zeiss OPMI PENTERO (Zeiss, Oberkochen, Germany), during aneurysm clipping. Representative intraoperative photographs of the aneurysm dome were extracted from the video data, and regions of the dome were divided into TIWRs and TKWRs based on the color and translucency of the aneurysm dome (Fig. 1, 2). TIWRs of aneurysms were defined as regions with a red color, a translucent appearance, and extreme wall thinness compared with healthy areas of the MCA<sup>8,9,10,13</sup>. In contrast, TKWRs of aneurysms were defined as regions with nonred coloring, including white and pink colors (similar to a normal parent artery), and yellowish arteriosclerotic lesions, as previously described<sup>11</sup>. In this study, we focused on regions of aneurysm wall thinning. Therefore, we did not distinguish between whitish normal-like colored walls and yellowish arteriosclerotic walls. The findings were assessed by 3 independent neurosurgeons.

### Three-Dimensional CT Angiography

Dynamic CT examinations were performed with a 320-detector row CT scanner (Aquilion ONE, Toshiba Medical Systems Corporation, Tokyo, Japan) using volumetric cine scanning without helical imaging. The technical parameters were as follows: 160×0.5-mm detector width; 0.25-mm reconstruction interval; 512×512 matrix; 180–240-mm field of view; tube voltage, 80 to 100 kV; tube current, 100 to 200 mAs; detector width, 80 mm; and a total of 20 scans. The scanning delay was automatically adjusted using a test injection method. Eighteen subsequent dynamic scans were acquired with continuous scanning at one scan rotation per 1 s, followed by two intermediate dynamic scans at one scan rotation per 5 s in the late venous phase. Twenty-five milliliters of nonionic contrast material (370 mgI/ml) was injected into the right cubital vein at a rate of 5 ml/s, followed by a 40-ml saline flush.

### Computational Fluid Dynamics

CTA raw data were transferred to an image processing workstation (Ziostation 2; Ziosoft Inc., Tokyo, Japan) for further image processing and analysis. In the Ziostation, Hemoscope Ver1.5 (EBM corp., Tokyo, Japan) was used for meshing, and a hemodynamic analysis was performed,

1 including visualization of the results as following manner. First, the vascular geometries were  
 2 filled with unstructured cells. The shapes mainly consisted of hexahedrons with sizes of  
 3 approximately 0.25 mm in the far-wall region and 0.125 mm (width) and 0.05 mm (height) in the  
 4 near-wall regions. Near-wall meshes consisted of 3 layers. The inlet and outlet vessels were  
 5 extended to 5- and 10-times greater than the measured diameters, respectively. The blood density  
 6 ( $\rho$ ) and viscosity ( $\mu$ ) were set at 1050 kg/m<sup>3</sup> and 0.004 Pa·s, respectively. The boundary conditions  
 7 were determined in accordance with the constant wall shear stress (WSS) theory. In other words,  
 8 the flow rates of the inlet and outlet vessels were calculated using the following equation:  $Q =$   
 9  $(\tau_w/32\mu) \times D^3$ , where  $Q$ ,  $\tau_w$ ,  $\mu$ , and  $D$  are the flow rate, WSS, fluid viscosity, and vascular diameter,  
 10 respectively. This equation is a well-known theoretical basis for fully developed laminar pipe flow.  
 11 In this study, the WSS ( $\tau_w$ ) was set to 1.5 Pa<sup>14</sup>. After calculating total inflow at the inlet vessel, the  
 12 amount of inflow was distributed to each outlet vessel according to the above equation, and the  
 13 specified boundary conditions of the inlet and outlet vessels were the pressure and velocity  
 14 boundary conditions, respectively. The present computation adopted unsteady flow, and the inlet  
 15 pressure was set to 100 mm Hg. A finite volume method was used to solve the governing equations:  
 16 3D unsteady Navier-Stokes equations and the equation of continuity. Blood was assumed to be an

incompressible and Newtonian fluid, and the nature of flow was allowed to have transient behaviors. The Euler and second-order upwind schemes were adopted for discretizing unsteady and convective acceleration terms. The convergent criteria were set to  $10^{-4}$ .

## Postprocessing

Computed velocity and geometry information allowed us to calculate the hemodynamic parameter WSS magnitude cycle average (WSSMA), which is equivalent to a common hemodynamic index time-averaged WSS (TAWSS), which is defined as

$$WSSMA = \frac{1}{T} \int_0^T |\boldsymbol{\tau}_t| dt$$

where  $T$  is the duration of the cardiac cycle, and  $\boldsymbol{\tau}_t$  is the WSS vector at time  $t$ , as described in previous studies<sup>15-16</sup>.

To quantify the magnitude of WSS oscillation, we computed the WSSVV by using Hemoscope, where WSSVV represents the summation of the directional change in the WSS in a cardiac cycle. WSSVV is defined as

$$WSSVV = \int_0^T \Delta\theta_t dt$$

where  $T$  is the duration of the cardiac cycle, and  $\Delta\theta_t$  is the directional change in WSS  $\boldsymbol{\tau}_t$  with

respect to time  $t$ . Here, note that the WSSVV was used in this study to assess the absolute effect of the directional changes in the WSS.

#### Optimal Color Bar Scaling to Discriminate TIWRs and TKWRs

For visualization of the computational results, the position and orientation of each CFD color map were adjusted to match those in the corresponding clinical images by referring to the characteristic shapes of the cerebral aneurysms and the locations of the parent arteries.

WSSMA and WSSVV were calculated with patient-specific color bar scaling, which is automatically assigned based on the patient's specific maximum WSSMA and WSSVV values; the median values were 13.77 (interquartile range 10.76 to 21.03) and 861.50 (interquartile range, 698.25 to 1010.22), respectively. In this study, we focused on WSSVV. We found that the primary CFD maps with WSSVV values were not suitable for predicting cerebral aneurysm wall conditions (Fig. 1). The most clearly distinguishable values between TIWRs and TKWRs seemed to vary from the default images. The maximum color bar value (MCBV) should be adjusted manually patient by patient to the optimal value to clearly distinguish TIWRs and TKWRs. For the universal application of color maps to predict TIWRs, we investigated the optimal MCBV, which was

determined by two methods.

One method is to calculate the mean MCBV. We selected one optimal MCBV between 300 and 700 at every 100 intervals for every aneurysm to capture the TIWRs and TKWRs by comparing the intraoperative images with the color maps of the WSSVV (Fig. 1). These values were ultimately used to calculate the mean of the optimal MCBVs.

Another method is to analyze the sensitivity and specificity of the WSSVV values for detecting the TIWRs of each aneurysm. Among 12 aneurysms, a thin red wall was observed in 18 regions (indicated by yellow circles in Fig. 2), and a relatively thick or a thick whitish or yellowish wall was observed in 16 regions (indicated by blue circles in Fig. 2). We assessed the accuracy of the correspondence between the blue region on the WSSVV color map and the thin red wall in every aneurysm wall at each color bar ranging between 300 and 700 by changing the MCBV step by step from 300 to 700 at every 100 intervals. By using the obtained sensitivity and specificity values, a receiver-operating characteristic (ROC) analysis was performed, and the value of the left-uppermost corner point was selected as the optimal value for the WSSVV and the prediction of TIWRs. During the process of these analyses, we found that an MCBV of 500 was likely optimal. Therefore, we performed additional assessments at maximum values of 450 and 550.

## Verification of the Difference in WSSVV Values between Thin and Thick Walls

Finally, we assessed significant differences in the quantitative WSSVV values between the blue and nonblue regions on the CFD maps, which corresponded to the thin and thick regions, respectively, at the optimal MCBV for WSSVV (obtained from the above methods). Hemoscope could not calculate the WSSVV values quantitatively for the selected arbitrary regions on the aneurysm domes. Therefore, we used ImageJ software (National Institutes of Health, Bethesda, Maryland) to convert the obtained color map images consisting of RGB colors into Hue images to quantitatively calculate the values in the selected regions on the WSSVV color maps, which also consisted of RGB colors. For example, the pure blue region in the color map was assigned a minimum value of zero, and the pure red region was assigned a maximum value of 255 (Fig. 3).

## Statistical Analysis

Continuous data are shown as the mean $\pm$ SD, and categorical variables are shown as percentages. Fisher's exact test was applied to analyze differences in categorical factors. We used the Mann-Whitney U test to compare continuous variables for which normality could not be established. All

1 statistical analyses were performed with EZR (Saitama Medical Center, Jichi Medical University,  
2 Saitama, Japan), a graphical user interface for R 3.4.3 (R Foundation for Statistical Computing,  
3 Vienna, Austria). EZR is a modified version of R commander (version 1.6-3) designed to add  
4 statistical functions that is frequently used in biostatistics. A  $p$ -value<0.05 was considered  
5 statistically significant. To detect the accuracy of predicting TIWRs, a ROC analysis was  
6 performed by using the sensitivity and specificity for every MCBV of the WSSVV.

## 8 RESULTS

### 9 Optimal Color Bar Scaling to Discriminate Thin and Thick Aneurysm Walls

#### 10 The Mean Value of the Optimal Maximum Color Bar Ranges

11 All selected TIWRs or TKWRs among the 12 aneurysms almost corresponded to the selected  
12 blue or nonblue areas of the WSSVV color maps, respectively, by adjusting the MCBVs (Fig. 4).  
13 The mean of the optimal MCBV was  $483.3 \pm 167.50$  (range, 300-700). However, the color map of  
14 the WSSMA did not detect TIWRs in all 12 aneurysms, which generally tended to have low WSS  
15 values throughout the aneurysm dome (Fig. 1, Fig. 4).



# 1 Analysis of the Optimal MCBVs with High Sensitivity and Specificity

2 At an MCBV of 300, 10 of 18 red, thin selected walls corresponded to the blue areas of the  
 3 WSSVV color map (sensitivity: 0.56). In contrast, all 16 white, thick selected walls corresponded  
 4 to the nonblue area of the WSSVV map (specificity: 1.00). At an MCBV of 400, 14 of 18 thin  
 5 selected walls and all 16 thick selected walls corresponded well to their respective areas  
 6 (sensitivity: 0.78, specificity: 1.00). At an MCBV of 450, 15 of 18 thin walls and 15 of 16 thick  
 7 walls corresponded well to their respective areas (sensitivity: 0.83, specificity: 0.94). At an MCBV  
 8 of 500, 16 of 18 thin walls and 15 of 16 thick walls corresponded well to their respective areas  
 9 (sensitivity: 0.89, specificity: 0.94). At an MCBV of 550, 16 of 18 thin walls and 13 of 16 thick  
 10 walls corresponded well to their respective areas (sensitivity: 0.89, specificity: 0.81). At an MCBV  
 11 of 600, 12 of 14 thin walls and 11 of 13 thick walls corresponded well to their respective areas  
 12 (sensitivity: 0.86, specificity: 0.85). At an MBCV of 700, 10 of 11 thin selected walls and 9 of 12  
 13 thick selected walls corresponded well to their respective areas (sensitivity: 0.91, specificity: 0.75).

14 A ROC analysis with these sensitivity and specificity values clarified that the optimal MCBV  
 15 was 500 (Fig. 5, Table 2), which was very similar to the mean optimal MCBV of 483.3, as  
 16 described above. Accordingly, we decided to use 500 as the optimal MCBV to predict aneurysm

wall conditions.

### Certification of the Differences in WSSVV Values between TIWRs and TKWRs

With the optimal MCBV set to 500, we calculated the Hue values in the regions of the WSSVV maps that corresponded to the TIWRs and TKWRs, respectively, under microscopy. The mean Hue values were  $103.7 \pm 21.3$  at red, thin walls and  $163.5 \pm 32.8$  at white, thick walls. This difference was statistically significant ( $p < 0.01$ ) (Fig. 6).

## DISCUSSION

In this study, we demonstrated that WSSVV is a reliable hemodynamic parameter that can be used to estimate aneurysm wall conditions, and the regions with low WSSVV corresponded to TIWRs on aneurysm walls. To the best of our knowledge, this is the first report to demonstrate that WSSVV is a reliable hemodynamic parameter that can be used to estimate the condition of an aneurysm wall, especially TIWRs, and we also certified these hemodynamic characteristics quantitatively with Hue values.

Regarding WSS, we could not find any relationship between WSSMA, which were equal to

TAWSS, and aneurysm wall thinning (Fig. 3). WSS did not show consistent results with respect to aneurysm wall conditions, which is consistent with previous reports<sup>10-12</sup>.

Regarding another prevailing hemodynamic parameter, high oscillatory shear index (OSI) have been reported to be associated with atherosclerosis in the aorta and carotid artery walls and cerebral aneurysms<sup>17-18</sup>. We presumed that atherosclerosis represents an opposite phenomenon to vessel wall thinning. Accordingly, we inferred that low OSI would be associated with aneurysm wall thinning, although no published articles support this conclusion.

The OSI is formulated to account for the cyclic departure of the WSS vector from its predominant axial alignment, which represents the degree of oscillation in the WSS vector in one cardiac cycle<sup>19, 20</sup>. WSSVV also represents the degree of oscillation on the WSS vector in one cardiac cycle. Accordingly, the OSI is a very similar parameter to WSSVV. Therefore, we focused on WSSVV.

WSS changes during one cardiac cycle with high oscillation in the WSS vector (corresponding to high OSI) result in damage to endothelial cells, thus activating a focal inflammatory process and leading to proliferation of endothelial cells, hypertrophic remodeling, and atherosclerosis<sup>21, 22-23</sup>. These processes may explain why high OSI values correspond to thickening of the cerebral

aneurysm wall. In contrast, low oscillation in the WSS vector, which indicates that the direction of the WSS vector is relatively constant with less oscillation during one cardiac cycle, does not activate focal inflammatory processes or cause hypertrophic remodeling. WSS is the frictional force applied by blood flowing tangentially on the vessel wall; originally, this force was thought to cause endothelial cell depletion and destructive remodeling followed by aneurysm initiation and rupture<sup>24, 25</sup>. Without oscillation of the WSS vector, the constant direction of the WSS may cause destructive remodeling followed by aneurysm wall thinning.

Unfortunately, even WSSVV is not a perfect parameter for estimating aneurysm wall thinning. In the current study, WSSVV could not accurately detect all the TIWRs within the aneurysm wall (sensitivity, 0.89; specificity, 0.94) (Fig. 5, Table 2). A combined analysis of WSSVV and other parameters, including pressure differences (PD) and impingement of blood flow, may yield a more reliable preoperative estimation of aneurysm wall thinning<sup>9, 26</sup>.

However, we concluded that Hemoscope was user friendly and relatively familiar to clinical medical doctors (unlike other commercially available CFD software). The analysis protocol is relatively simple, and clinicians can operate Hemoscope without assistance from an engineer<sup>15, 27-28</sup>. We have been working with our colleagues in the mechanical engineering division of our

1 university to develop another CFD tool, and the results of this current study have been discussed  
2 with them. However, all analysis procedures in the current study can be performed by clinicians  
3 without assistance from an engineer.

4 Although Hemoscope cannot measure the OSI, PD or other specific parameters directly, it could  
5 provide the basic parameter WSSVV, which identified the TIWRs of cerebral aneurysms with  
6 acceptable accuracy and will help clinicians (on site) perform safer surgery when treating cerebral  
7 aneurysms by clipping or coiling.

## 8 9 Limitations

10 The present study has some limitations. First, the comparisons between intraoperative views  
11 and CFD maps were conducted retrospectively after surgery. To verify the accuracy of detecting  
12 TIWRs, further prospective studies should be carried out. Second, TIWR was defined as regions  
13 with a red color, a translucent appearance areas of the aneurysm dome in the microscopic view in  
14 accordance with the previously reported method<sup>8, 9, 10, 11</sup>. This was a subjective method as well as  
15 the determination of thick white or yellowish walls ; a more objective evaluation method is  
16 necessary<sup>11</sup>. Furthermore, they have not been determined histopathologically. Investigation with

the specimen of TIWR and TKWR and the measurement of the wall thickness should be carried out for the confirmation of our results. Then we could see the destructive or hypertrophic remodeling in the specimen and evaluate a possible effect of WSSVV toward TIWR and TKWR.

Third, matching of the aneurysmal shape (on the CFD color map) to the clinical images was performed manually. Completely matching the aneurysmal shapes on the CFD color maps and the clinical images was difficult because the clinical images showed the appearance of aneurysms during microsurgery, but the blood vessel shapes on the CFD color maps were lumens reconstructed from the 3D-CTA data. Fourth, all CFD simulations employed the same boundary conditions, whereas in practice, these conditions may vary among cases. For patient-specific analyses, boundary conditions should be established with magnetic resonance imaging and echocardiographic imaging, if available. Fifth, the vessel walls were assumed to be rigid, whereas in practice, they may deform to different degrees during the cardiac cycle. However, previous investigators have indicated that these are second-order issues with only minimal effects on flow dynamics, and the most important factor is actual vessel geometry<sup>29, 30</sup>. Finally, the present study was performed with a small number of cases. Therefore, further prospective studies with additional cases are warranted.

1

## 2 CONCLUSIONS

3 Low WSSVV values on an aneurysm wall possibly indicate TIWRs. Preoperative simulation  
4 using CFD and predicting TIWRs may help to avoid procedure-related, unintentional  
5 intraoperative rupture not only during microsurgical clipping but also during endovascular coiling.

6

## 7 ACKNOWLEDGMENTS

8 We would like to thank Prof. Takashi Ohmori of the Clinical & Translational Research Center,  
9 Kobe University Hospital; Mr. Noriyuki Negi of the Division of Radiology, Department of  
10 Medical Technology, Kobe University Hospital; and Mr. Hiroshi Inoue of AMIN corp. for their  
11 analytical support with the R-commander, the CTA data and Hemoscope data, respectively.

12

## 13 FUNDING

14 This research did not receive any specific grant from funding agencies in the public, commercial,  
15 or not-for-profit sectors.

## 1    **FIGURE LEGENDS**

2    Fig. 1 A 55-year-old woman, right middle cerebral aneurysm. A: Intraoperative microscopic image  
 3    of an unruptured saccular aneurysm. B: Wall shear stress magnitude cycle average (WSSMA), C-  
 4    J: Wall shear stress vector cycle variation (WSSVV) at maximum color bar value (MCBV) of the  
 5    original value (C), 300 (D), 400 (E), 450 (F), 500 (G), 550 (H), 600 (I), and 700 (J). A selected  
 6    thin-walled region (TIWR) (blue dotted circle, A) and a thick-walled region (TKWR) (green dotted  
 7    circle, A) within an aneurysm dome could not be distinguished by the WSSMA color map (B), in  
 8    which both corresponding regions had blue areas (yellow dotted circle and red dotted circle,  
 9    respectively), B) but they could be detected by the WSSVV color map (C), in which the former  
 10    had blue area (yellow dotted circle) and the latter had green area (red dotted circle) of the WSSVV  
 11    color map not only at the original MCBV (C) but also at any MCBV (D-J) in this case. When the  
 12    MCBV was set to a higher value (from D to J), the blue area on the aneurysm dome became wider,  
 13    indicating that the estimated thin-walled region became larger. In contrast, when the MCBV was  
 14    set to a smaller value (from J to D), the blue area on the WSSVV map decreased, and the green-  
 15    yellow area become larger, indicating that the estimated thick-walled region on the aneurysm dome  
 16    became larger. Accordingly, in order to detect the optimal MCBV, the MCBV should be adjusted



manually to the most clearly distinguishable value of the TIWRs and TKWRs for each patient by visually comparing the actual intraoperative microscopic images with the WSSVV maps over the whole aneurysm dome. In this case, the optimal MCBV was determined as 300 because TIWRs and TKWRs within the whole aneurysm dome could be distinguished most clearly at an MCBV of 300. For example, the relative TKWR (black dotted circle) had the greenest area on the WSSVV color map at an MCBV of 300 (D), indicating the TKWR among the corresponded areas (white dotted circle, D-J).

(MCBV, maximum color bar value; TIWRs, thin-walled regions; TKWRs, thick-walled regions; WSSMA, wall shear stress magnitude cycle average; WSSVV, wall shear stress vector cycle variation)

Fig. 2 The selected 18 thin-walled regions (yellow circles) and 16 thick-walled regions (blue circles) among 12 aneurysms for the sensitivity and specificity analysis of WSSVV.

(WSSVV, wall shear stress vector cycle variation)

Fig. 3 Illustration showing the quantitative analysis of a WSSVV color map image using ImageJ

1 (National Institutes of Health, Bethesda, Maryland) for a left middle cerebral artery aneurysm in a  
 2 57-year-old woman. RGB (red, green, blue) color images of WSSVV (A) were converted to HSB  
 3 (hue, saturation, brightness) colors in ImageJ. To set the maximum value of pure red to 255 and  
 4 the minimum value of pure blue to zero, the Hue image (left in B) was inverted (C). By using this  
 5 inverted image, an image consisting of RGB colors can be analyzed sequentially from zero to 255  
 6 with progression from blue to red. D: The upper row shows a selected thin-walled region (yellow  
 7 circle) in the operative view (left), an RGB color map of the WSSVV (middle), and an inverted  
 8 Hue image (left). The lower row shows a selected thick-walled region (yellow circle) in the  
 9 operative view (left), an RGB color map of the WSSVV (middle), and an inverted Hue image (left)  
 10 (the inset table shows the calculated mean (right), minimum (middle), and maximum (left) Hue  
 11 values of the selected area).

12 (WSSVV, wall shear stress vector cycle variation)

13

14 Fig. 4 All twelve aneurysms' intraoperative views (left column), WSSVV color maps (mid column),  
 15 and WSS magnitude cycle averages (right column). The thin-walled region of each aneurysm dome  
 16 (blue dotted circle) in the intraoperative view had a low WSSVV value (yellow dotted circle), and

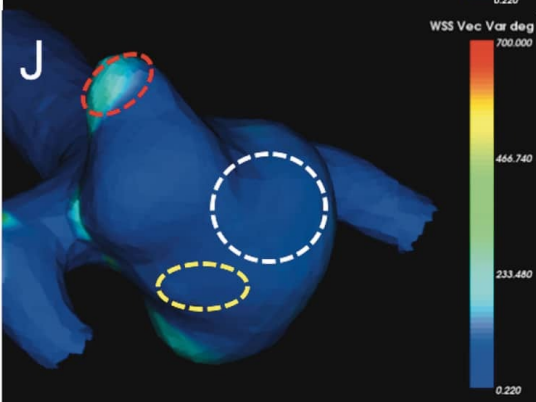
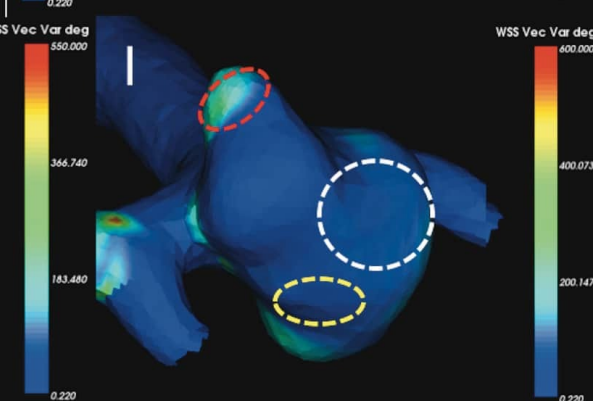
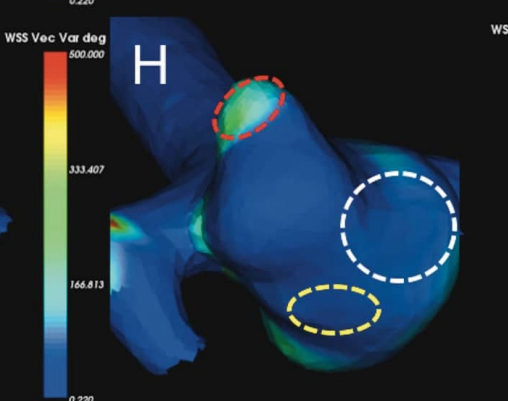
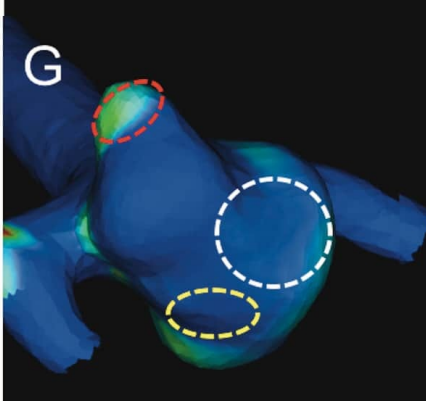
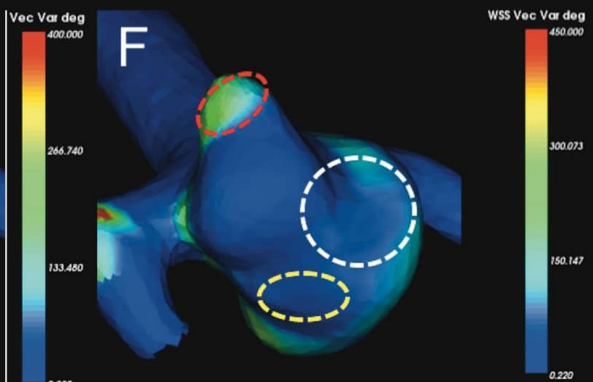
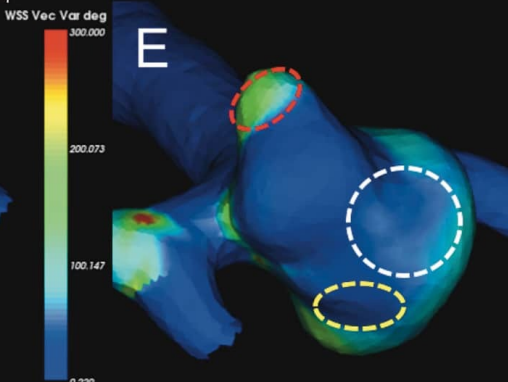
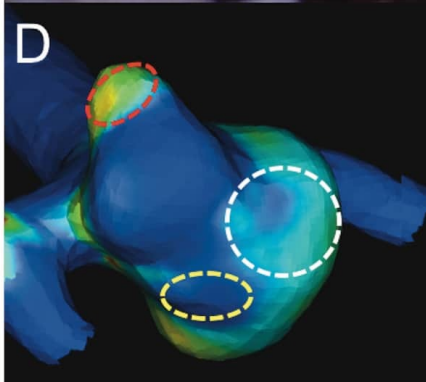
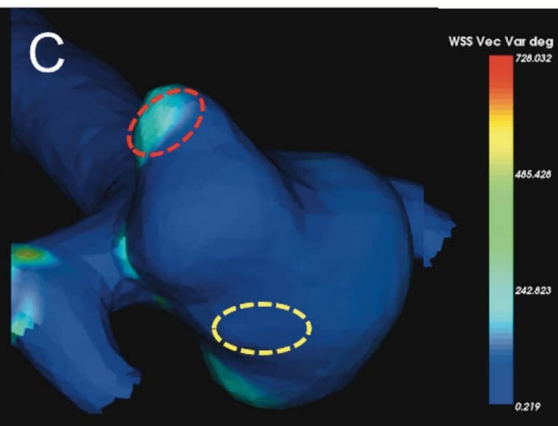
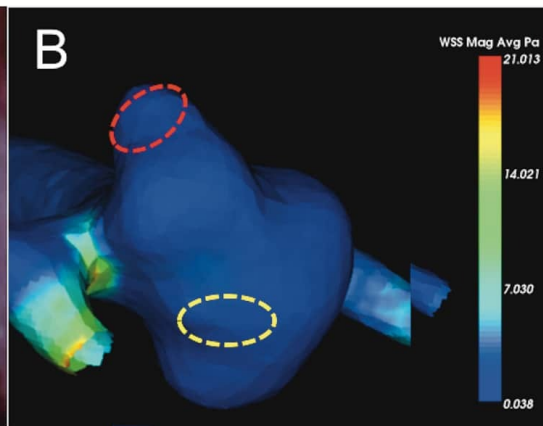
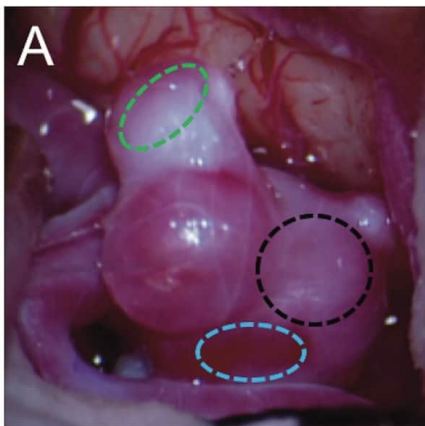
the thick-walled region (green dotted circle) had high WSSVV values (red dotted circle) under the adjusted optimal maximum color bar range (from a top case to a bottom case; 300, 500, 300, 600, 300, 700, 600, 700, 700, 500, 300, and 300 in order). The WSS magnitude cycle average could not detect any thinned regions in the aneurysm walls.

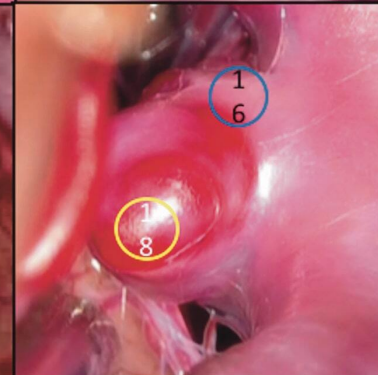
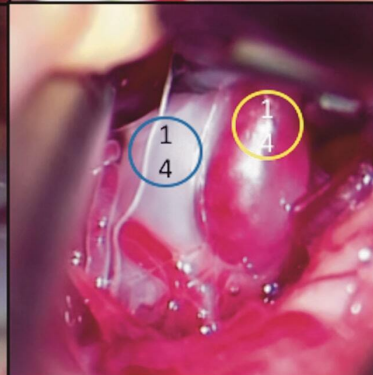
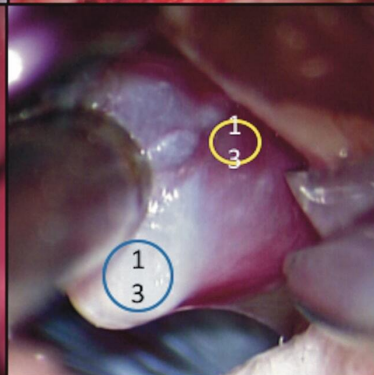
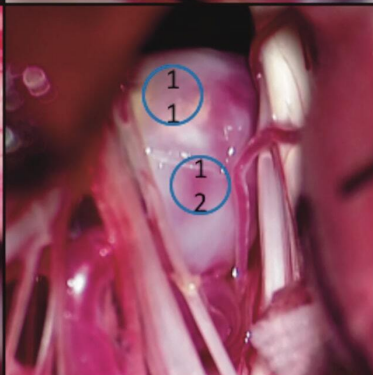
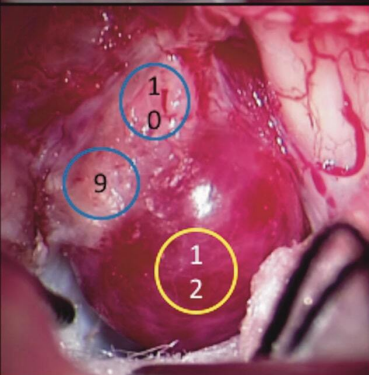
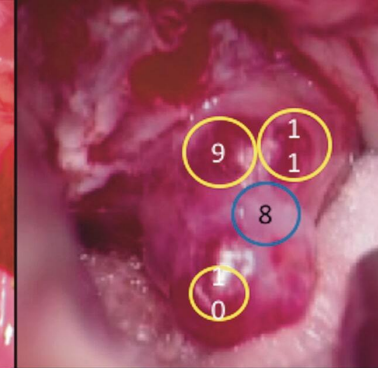
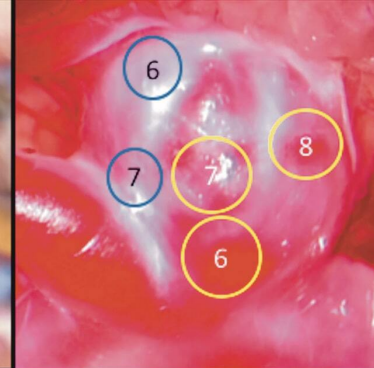
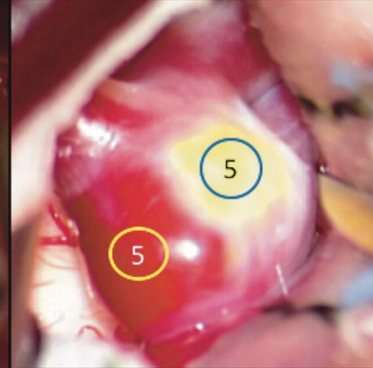
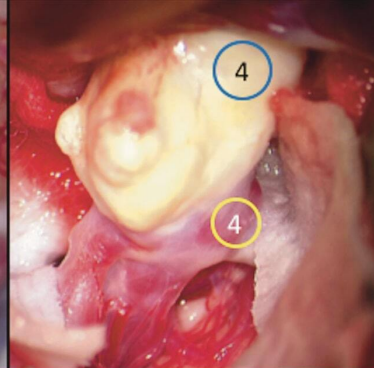
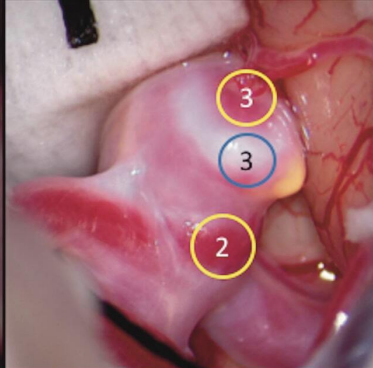
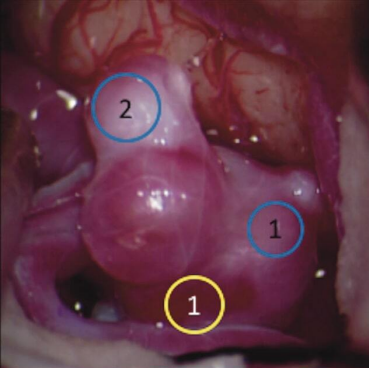
(WSSVV, wall shear stress vector cycle variation)

Fig. 5 A receiver-operating characteristic analysis with obtained sensitivity and specificity values at a maximum range of 300 to 700 at every 100 intervals and an additional assessment within the range of 450 and 550. The arrow shows the value of the left-uppermost corner point, which was analyzed as 500 with a sensitivity of 0.89 and a specificity of 0.94 (Table 2).

Fig. 6 Hue values of each region on the WSSVV color maps corresponding to TIWRs and TKWRs. The mean Hue values were  $103.7 \pm 21.3$  at TIWRs and  $163.5 \pm 32.8$  at TKWRs. This difference was statistically significant ( $p < 0.01$ ).

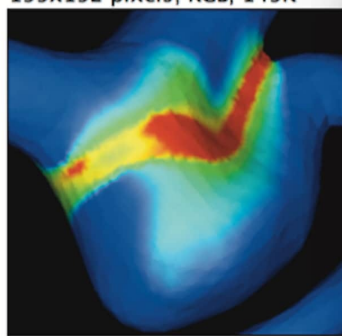
(TIWRs, thin-walled regions; TKWRs, thick-walled regions; WSSVV, wall shear stress vector cycle variation)







A 199x192 pixels; RGB; 149K

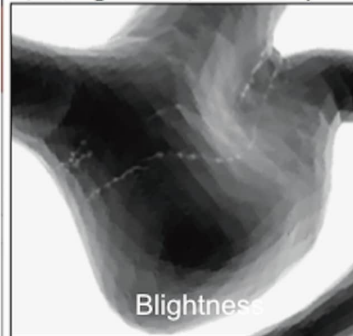
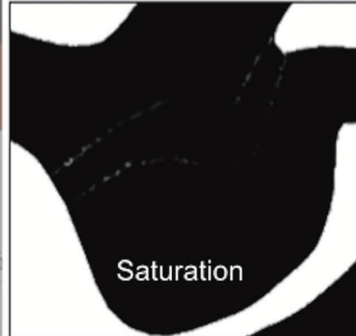


HSB Stack

B

Hue

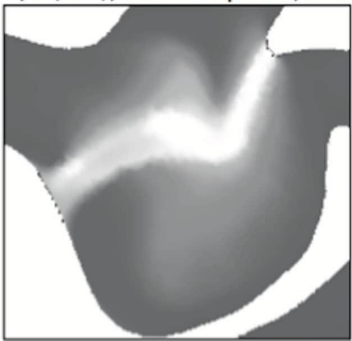
1/3 (Hue); 199x192 pixels; 8-bit 2/3 (Saturation); 199x192 pixels 3/3 (Brightness); 199x192 pixels



C

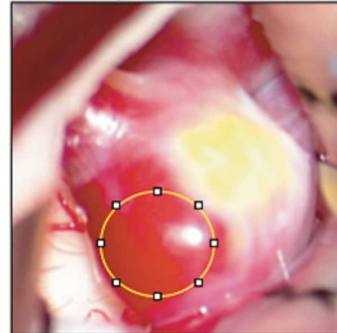
Invert

1/3 (Hue); 199x192 pixels; 8-bit

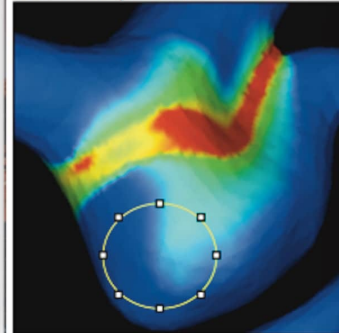


D

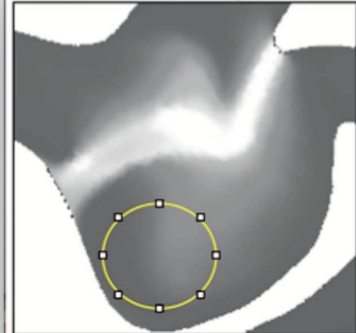
193x192 pixels; RGB; 145K



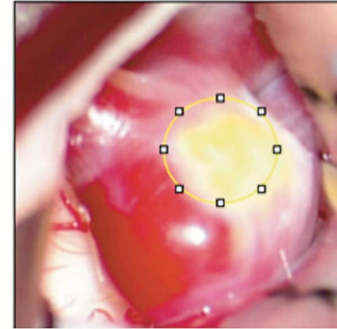
199x192 pixels; RGB; 149K



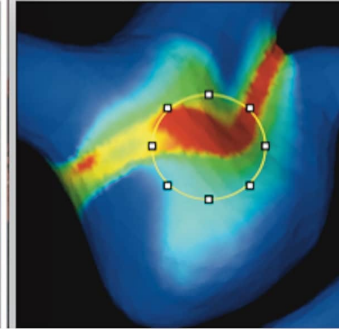
1/3 (Hue); 199x192 pixels; 8-bit



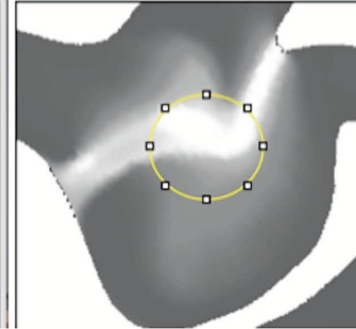
193x192 pixels; RGB; 145K



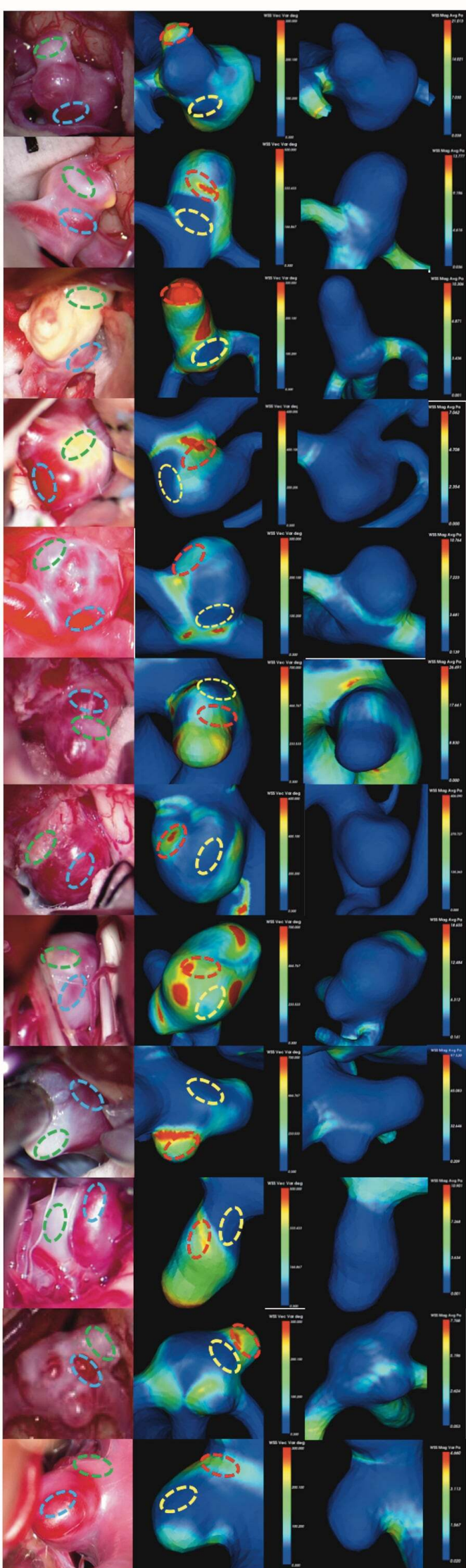
199x192 pixels; RGB; 149K

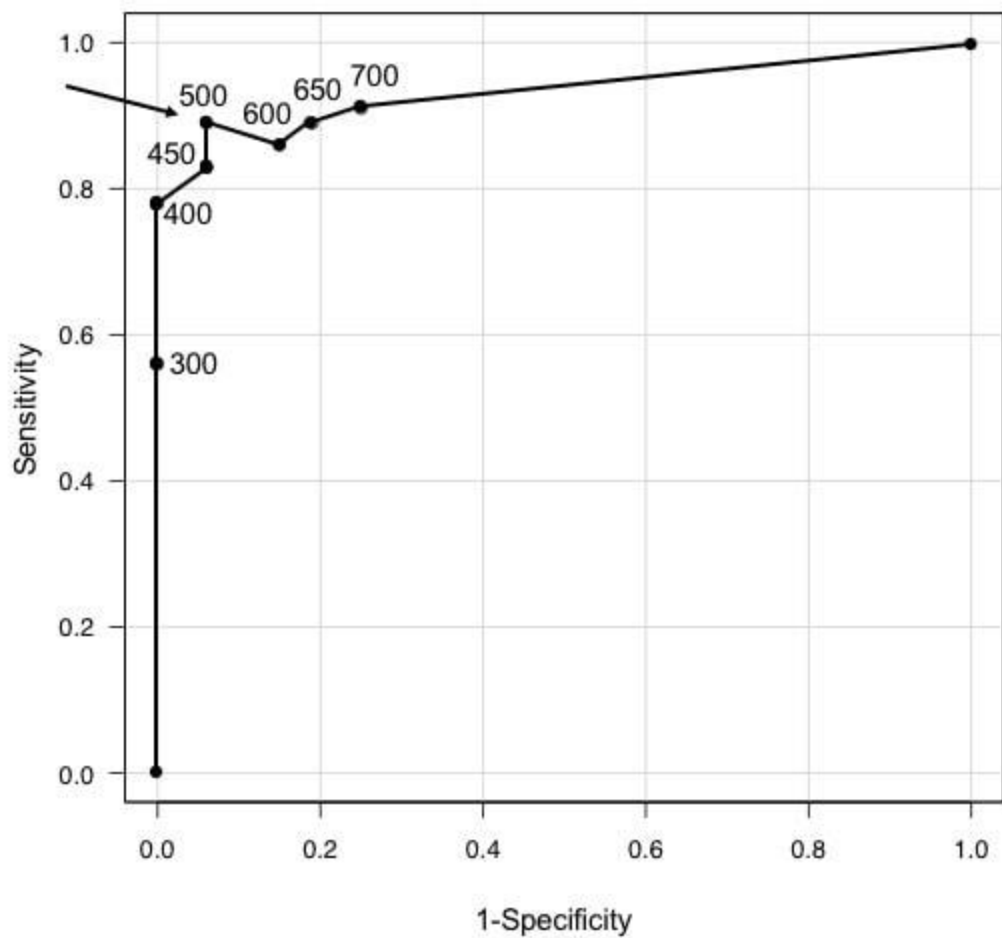


1/3 (Hue); 199x192 pixels; 8-bit



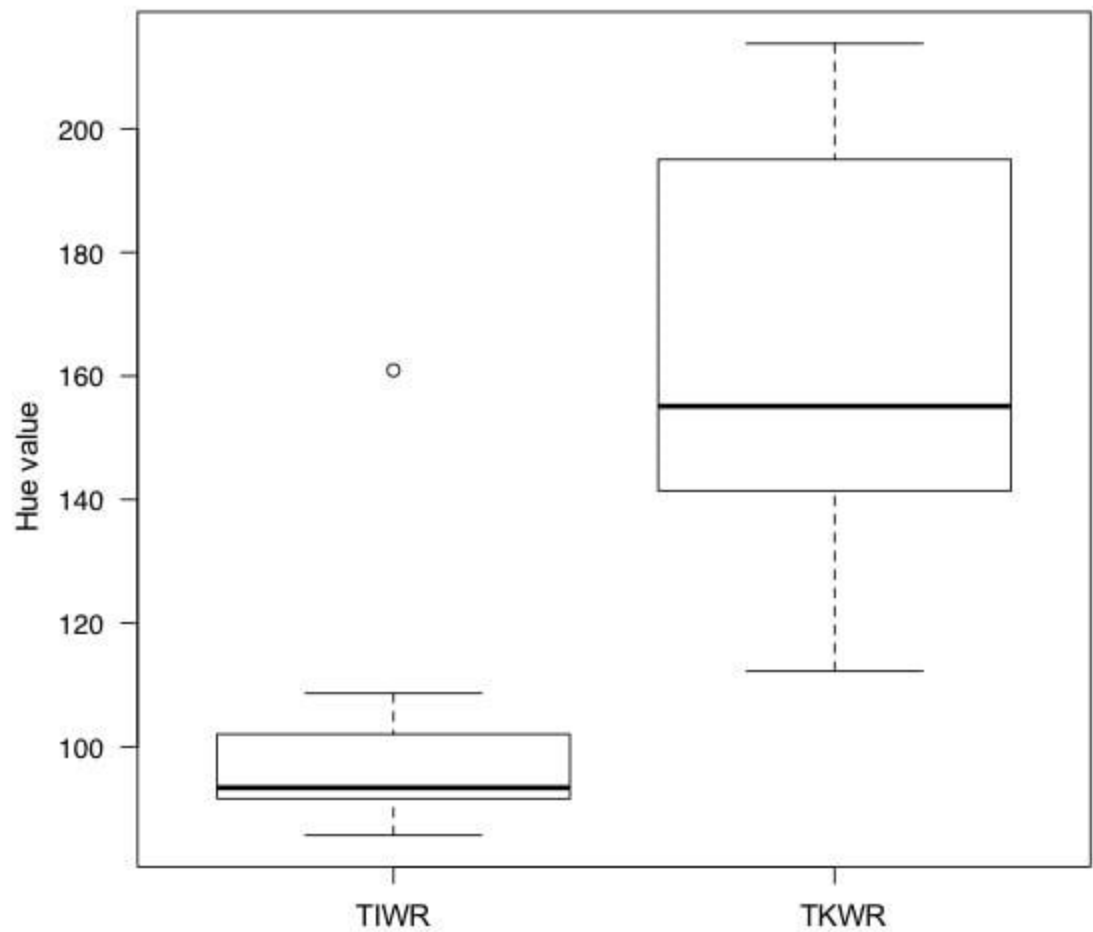
	Mean	Min	Max
thin wall	102.921	85	129
thick wall	199.056	119	255







$P < 0.01$



Case	Age (years)	Sex	R/L	Location	Max dome size (mm)
1	55	F	R	MCA	7.5
2	50	M	L	ICA	4.8
3	61	M	R	MCA	8.8
4	68	F	R	MCA	6.5
5	57	F	L	MCA	7.3
6	73	F	R	MCA	6
7	51	F	L	ICA	4.8
8	68	F	L	VA	6.8
9	80	F	R	ICA	5.5
10	47	F	L	ICA	6.8
11	64	F	R	MCA	5.4
12	70	M	L	ICA	5

WSSVV: 0-	300	400	450	500	550	600	700	
Sensitivity	0.56	0.78	0.83	0.89	0.89	0.86	0.91	
Specificity	1	1	0.94	0.94	0.81	0.85	0.75	
P	p=0.0004	p=0.0000	p=0.0000	p=0.0000	p=0.0001	p=0.0004	p=0.0028	<0.05
(Fisher's exact test)								